Proc. Schl. Eng. Tokai Univ., Ser. E
37 (2012) 19-22

Forced Vibration Analysis of a Model Structure with New Tuned Cradle Mass Damper

by

Witsanu MUNFAK[*1] and Yoji SHIMAZAKI[*2]

(Received on Mar. 20, 2012 and accepted on May 17, 2012)

Abstract

A tuned cradle mass damper (TCMD) relies on the motion of a swing mass on a curved surface to dissipate structural vibration energy. This study obtained the constant swing speed of the TCMD for large swing amplitudes and verified the performance of the new TCMD through both experiments and numerical analyses of the structure under forced vibration. To obtain the constant speed of the device, the variable radii of the curved surfaces were calculated using simple pendulum dynamics. For this study, the damper was installed on a frame model of a simple one-story structure with a frequency of approximately 1 Hz and excited under forced vibration. The results obtained by the numerical analyses agreed well with those of the experiments. Numerical analyses under harmonically excited and El Centro earthquake (1940) motions of the structure were performed to verify the effect of the TCMD. The TCMD significantly reduced the displacement response of the structure.

Keywords: vibration control, tuned mass damper, forced vibration

1. Introduction

Structures vibrate due to forces such as earthquakes, wind, and the forces accompanying human activities, including civil engineering work, building work and moving transportation vehicles. Because the damping performance of a structure itself is generally weak, when a natural vibration mode of the structure resonates with dynamic external force, the response of the structure is amplified and various problems such as decreased livability or damage to the structure can occur. The reason for these problems is that only a static load such as a dead load is considered in a conventional design, and the vibration characteristics of the structure or the dynamic external forces are not considered.

In such vibration problems, application of vibration control systems has been performed. Vibration control systems are classified broadly into passive and active types. The mass body of the passive type vibration control system automatically responds to the vibration of structure and reduces it. The active type vibration control system detects the vibration of the structure, activates a mass body responding to the vibration of the structure effectively, and controls it. An electric or hydraulic actuator is used for activation of the mass body.

The objectives of this study are to obtain the constant swing speed of the tuned cradle mass damper (TCMD) for large swing amplitudes and to verify the performance of the new TCMD through both experiments and numerical analyses when a structure is under forced vibration. To obtain the constant speed of the device, the variable radii of the curved surfaces were calculated using simple pendulum dynamics. For this study, the damper was installed on a frame model of a simple one-story structure with a frequency of approximately 1 Hz and excited in forced vibration. Numerical analyses under harmonically excited and El Centro earthquake (1940) motions of the structure were performed to verify the effect of the TCMD.

2. Device Configuration

2.1 Experimental Model

To examine the cradle type TCMD experimentally, a model of a one-story structure is used. Figure 1 shows the model, which is made of steel columns 1300 mm in length, 60 mm in width, and 8 mm in thickness. Four columns support a floor. The lateral spring constant of the structure,

*1 Graduate Student, Course of Civil Engineering
*2 Professor, Department of Civil Engineering

k_1 , is 11.1 kgf/cm. Figure 2 shows that the force-displacement relationship of the structure for the effective mass of the structure is approximately 220 kg. The natural frequency of the structure is 1.12 Hz. Figure 3 shows the displacement response of the structure in the uncontrolled condition. The initial lateral displacement given to the structure is 12 mm. The damping constant of the structure calculated between the two marker points in Figure 3 is 0.0013.

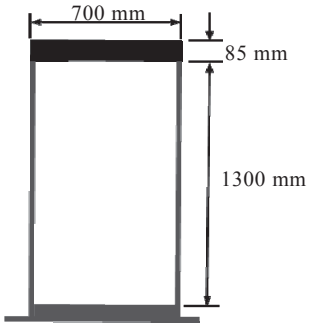

Fig.1 Simple structure model.

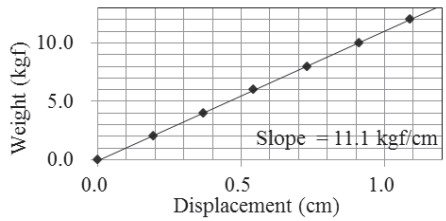

Fig.2 Force-displacement line of the structure.

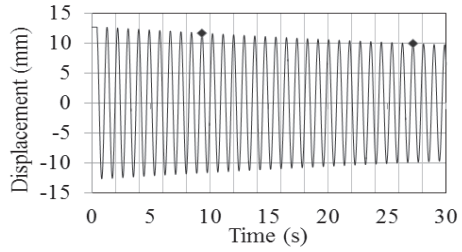

Fig.3 Free vibration of the structure.

2.2 Modeling of the TCMD

Figure 4 shows the TCMD used in the experiments. The TCMD is made of three copper plates with the swing mass having three wheels. The size of the middle plate is $500 \times 280 \times 5$ mm and the two side plates are $710 \times 280 \times 5$ mm. The diameter of each wheel is 72 mm. The swing mass including the wheels is approximately 6 kg. The mass moves along three curved surfaces as the structure moves. To obtain magnetic damping [1, 2], neodymium magnets are attached to both sides of the swing mass. The magnetic field then develops when the mass moves along the copper plates. The damping strength of the mass can be adjusted by varying the number of magnets attached to the swing mass.

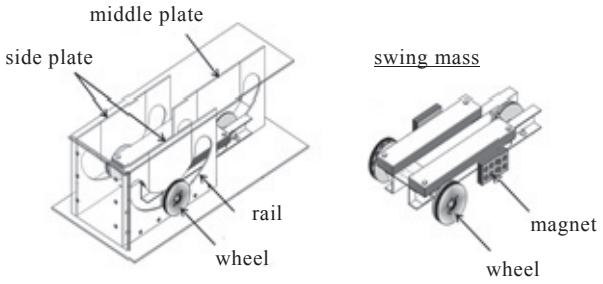

Fig.4 Tuned cradle mass damper.

Figure 5 shows the relationship between the number of magnets used for the TCMD and the corresponding damping constant h_2. Here, h_2 is the damping constant obtained from the free vibration of the TCMD. The natural frequency of the TCMD is 1.19 Hz and is constant for large amplitudes of the mass swing. The constant swing mass speed can be adjusted by modifying the curve radius surfaces explained in the next section. The damping constant h_2 = 7.0 % is used for the forced vibration experiment.

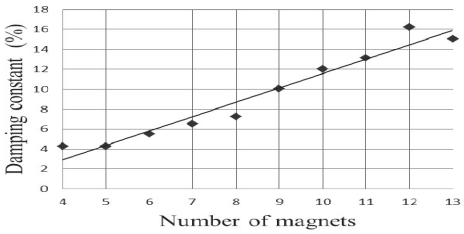

Fig.5 Number of magnets versus damping constant h_2.

3. Numerical Analysis Model

3.1 Determination of the variable radii

The differential equation for motion of a simple pendulum without damping force is as follows.

$$\frac{d^2\theta}{dt^2} + \frac{g}{\ell_p}\sin\theta = 0 \tag{1}$$

where g is the acceleration due to gravity, ℓ_p is the length of the pendulum, t is the time, and θ is the angular displacement. The period T_p for the motion described in eq. (1) is given by

$$T_p = 4\sqrt{\frac{\ell_p}{g}}K \tag{2}$$

where $$K = \int_0^{\pi/2} \frac{d\varphi}{\sqrt{1-\sin^2(\theta_m/2)\sin^2\varphi}} \tag{3}$$

In eq. (3), θ_m is the maximum swing angle of the pendulum. To obtain a constant T_p for large oscillation amplitudes, we can rewrite eq. (2) for ℓ_p as

$$\ell_p = \left(\frac{T_p}{4K}\right)^2 \cdot g \tag{4}$$

We calculate variable radii ℓ_p for each θ_m. Simpson's rule is used to integrate eq. (3). To obtain a constant speed of the TCMD, the variable radii ℓ_p are used to design the curved surfaces.

3.2 Forced vibration experiments of the structure

Figure 6 shows the free body diagram of the TCMD. Here, m_2 is the mass of the swing, θ is the angle of the oscillation, and ℓ_p is the variable radii at the angle θ. Because the mass of the wheels is small compared to the swing mass itself, we do not take the rotational energy by the wheels into account.

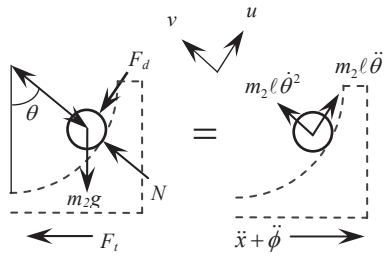

Fig.6 Free body diagram of the TCMD.

In addition, F_t is the horizontal force given by the TCMD, $\ddot{x}_2$ is the horizontal acceleration supplied by the structure, F_d is the damping force, N is the normal force, and ϕ is the ground motion. The equation of motion of the mass m_2 in the u and v directions can be written as

u direction: $$-m_2 g \cdot \sin\theta - F_d = m_2 \ell_p \ddot{\theta} \tag{5}$$

v direction: $$-m_2 g \cdot \cos\theta - N = m_2 \ell_p \dot{\theta}^2 \tag{6}$$

where $$F_d = c_2 \ell_p \dot{\theta} \quad . \tag{7}$$

Only the viscous damping c_2 is considered here. For simplicity, we do not take the frictional damping between the wheels and the curved surface into account. Then, the equations of the cradle in the horizontal direction become

$$F_d = c_2 \ell_p \dot{\theta}, \text{ where } \quad F_t = N \cdot \sin\theta + F_d \cdot \cos\theta \tag{8}$$

or $$\ddot{x}_2 = -\ell_p \dot{\theta}^2 \cdot \sin\theta - \frac{1}{m_2} c_2 \ell_p \dot{\theta} \cdot \cos\theta - g \cdot \cos\theta \sin\theta - \ddot{\phi} \tag{9}$$

Figure 7 shows the schematic figure of the structure. Here, m_1 is the mass, c_1 is the viscous damping coefficient, k_1 is the spring constant, and x_1 is the horizontal displacement of the structure. We then obtain the following equations of motion for the structure.

$$-F_t + c_1\dot{x} + k_1 x_1 = -m_1(\ddot{x}_1 + \ddot{\phi}) \tag{10}$$

or $$\ddot{x}_1 = -\frac{c_1}{m_1}\dot{x}_1 - \frac{k}{m_1}x_1 + \frac{m_2}{m_1}\ell_p\dot{\theta}^2 \cdot \sin\theta + \frac{m_2}{m_1} g \cdot \cos\theta \sin\theta + \frac{c_2 \ell_p \dot{\theta}}{m_1}\cos\theta - \ddot{\phi} \tag{11}$$

We now calculate the coupled equations (9) and (11) numerically.

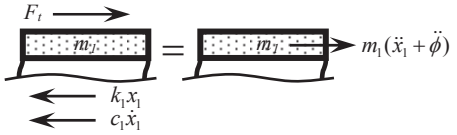

Fig.7 Free body diagram of the structure.

4. Results of the Experiments

4.1 Experimental Method

Experimental measurements are made to clarify the dissipation of vibration energy of the simple model structure by the TCMD action. Laser displacement sensors are used to measure both the time-displacement responses of the structure and the TCMD.

4.2 Forced vibration experiments of the structure

Figure 8 shows the resonance curves of the structure with and without the TCMD. The horizontal axis represents the frequency ratio and the vertical axis represents the displacement. As shown in the figure, the TCMD has a good damping effect on the model structure. Figure 9 shows the resonance curve of the structure with the TCMD and the TCMD only. The TCMD moves with approximately 3.5 times as much displacement as the structure does.

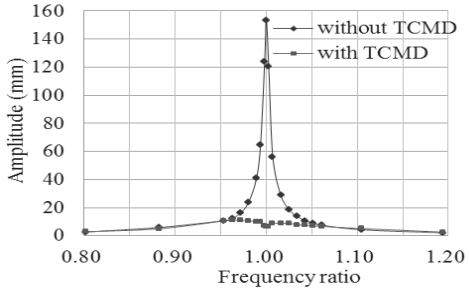

Fig.8 Resonance curve of the structure.

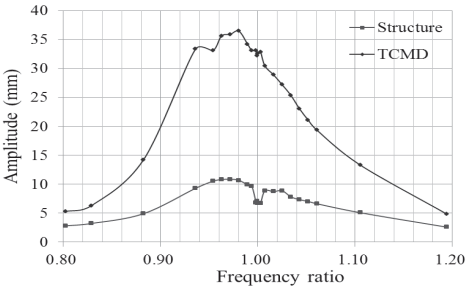

Fig.9 Resonance curve of the structure and the TCMD.

5. RESULTS OF THE ANALYSES

To solve eqs. (9) and (11), a fourth-order Runge-Kutta method is applied and is updated during every iteration time step. Figure 10 shows comparisons of the results obtained by the experiments and those by the analyses when the structure is under harmonically excited motion. Figure 11 shows the response of both the TCMD and the structure for the various viscous damping coefficients of the TCMD. The horizontal axis in Figure 11 represents the frequency ratio and the vertical axis represents the amplitude. As shown, all response curves of the structure intersect at the two points P and Q, [3]. The results obtained by the numerical analyses agree well with those of the experiments.

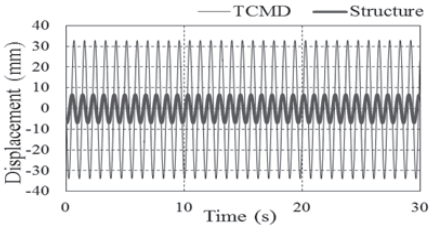

(a) Experiments

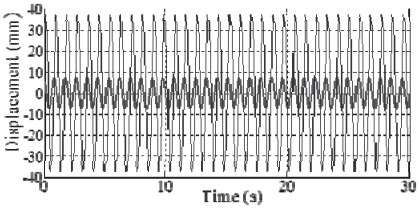

(b) Analyses

Fig.10 Response of TCMD and structure

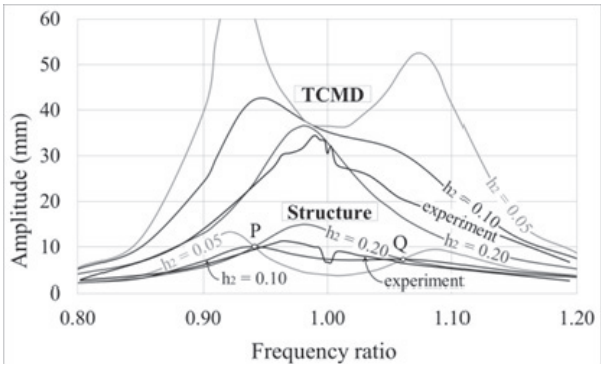

Fig.11 The TCMD and the structure response.

To demonstrate the TCMD effect under earthquake excitation, the El Centro earthquake (1940) is used for calculation. One-tenth of the actual acceleration is applied to calculate the displacement response of the structure. Figure 12 shows the displacement response waveforms obtained by the analysis. Figure 12(a) is the displacement response of the structure without the TCMD, (b) is the displacement response of the structure with the TCMD, and (c) is the displacement response of the TCMD only. We observe that the maximum displacement response caused by the El Centro earthquake in the structure with TCMD was reduced below the level of that in the structure without TCMD by approximately 50%.

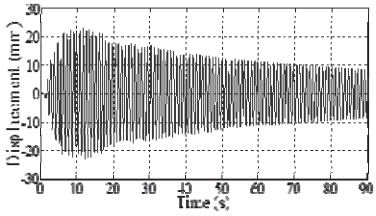

(a) Response of the structure without a damper

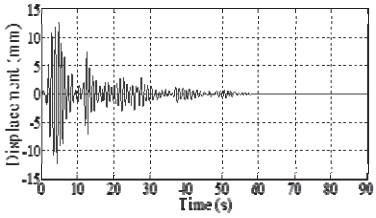

(b) Response of the structure with the TCMD

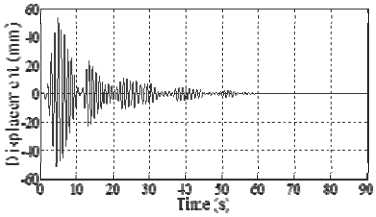

(c) Response of the TCMD only

Fig.12 Responses of the TCMD due to the El Centro earthquake.

It should be noted that the response of the TCMD is 4 times larger than that of the structure.

6. Conclusion

A new mechanical vibration absorber, called the tuned cradle mass damper (TCMD), is investigated in this study. This TCMD has a simple construction and is applicable to structures which may vibrate in lower frequency modes. The equation of reciprocal motion between the TCMD and the structure is derived to ensure the effectiveness of the TCMD. It is shown both experimentally and numerically that the new TCMD can efficiently dissipate undesirable vibration energy in a structure within the range of elastic deformation.

REFERENCES

1) Obata, M., & Shimazaki, Y. 2008. Optimum parametric studies on tuned rotary damped mass damper. Journal of Vibration and Control 14(6), 867-884.

2) Takei, H., & Shimazaki, Y. 2010. Vibration control effects of tuned cradle damped mass damper. Journal of Applied Mechanics 13, 587-594.

3) Den Hartog, J. P. 1956. Mechanical Vibration, McGraw-Hill, New York.